1 Response to Reviewer 3

1.1 Specific Comments

Reviewer comment: Table 1: Please add advantages and disadvantages of each product in the table.
Response:
In the revised version, the ‘Description’ column is removed and objective information (spatial/temporal resolution, temporal coverage, retrieval method) are included instead. The advantage/disadvantage of each product is included in main text.

Reviewer comment: P4, L 104: Please Just give some short explanation, as we don’t see the paper ready to submit
Response:
The following is added to the revised version: Using Shapley value to interpret different SciML models trained using the synthetic dataset, it was found that models with good performance have learned the spectral difference between snow, ice and water pixels.

Reviewer comment: Please make data section and explain satellite used for the retrieval, validation dataset, comparison dataset before methodology.
Response:
We appreciate this suggestion. The revised version includes a ‘Data’ section that separates the backgrounds of satellite and validation data sources from the discussion of the results.

Reviewer comment: Section 2.2: I would be merited to have a flowchart to understand better.
Response:
We are grateful for the suggestion. A flowchart has been included (Fig. 1) in the revised version.

Reviewer comment: Section 2.4: The details of structure of MLANN must be addressed. For example, the number of layers, activation functions, weight initialization, input variables (should be synthetic dataset, SD), target variables, how to train and validate, accuracies.
Response:
The following text has been added to the revised version.
The adaptive moment estimation (Adam) was chosen to update weights and biases in an MLANN, which is trained in 200 epochs with a batch size of 64.

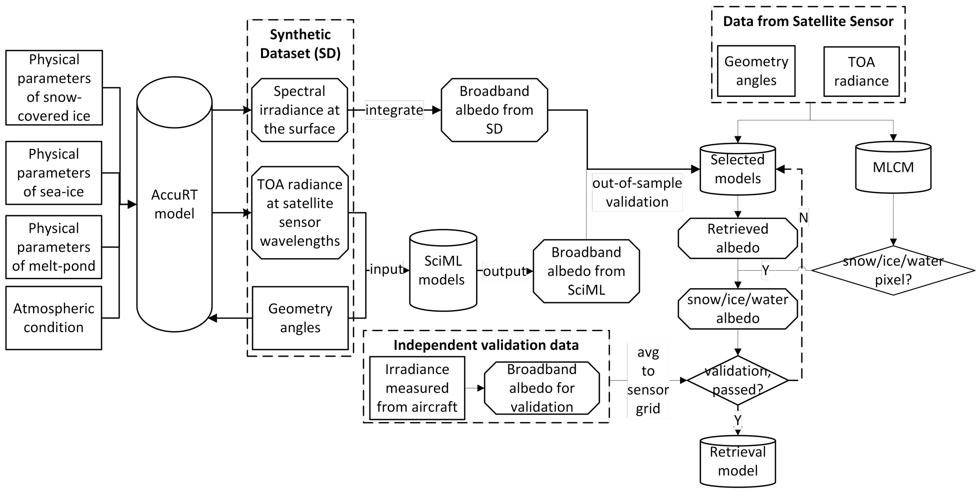

Figure 1: Flowchart of the proposed RTM/SciML framework for albedo retrieval.

A MLANN's hyperparameters include the learning rate and the activation function. To determine the optimal learning rate, Bayesian optimization was employed, and the Rectified Linear Units (ReLU) were used as the activation function in the hidden layers. Batch normalization is performed to enhance the MLANN's generalization capabilities and make the network less sensitive to random initialization of the weights and biases. To avoid overfitting, dropout layers were included as a regularization for networks with more than two hidden layers. In our evaluation, dropout layers with a rate of 0.2 were optimal, implying that one in every five inputs is randomly eliminated from each update cycle. A hidden-layer structure of $(16 \times 10 \times 8)$ was found to perform effectively with input data from both SGLI and MODIS sensors.

Reviewer comment: P10, L251: the cloud screening method used MODIS bands? If it's right, how can it be used for SGLI?
Response:
The cloud screening and surface classification model is also sensor-agnostic. Table 1 is added in the revised version to clarify.

Reviewer comment: Figure 2: This figure should go data section.
Response:
Moved.

Reviewer comment: Figure 3: Can you explain what is the difference

SGLI channels			MODIS channels		
λ	albedo	cloud mask	λ	albedo	cloud mask
380		x			
443	x	x	469	x	x
530	x	x	555	x	x
673.5		x	645	x	x
868.5	x	x	858.5	x	x
1050	x	x	1240	x	x
1630	x	x	1640	x	x
2210	x	x	2130	x	x

Table 1: Central wavelengths used by SGLI and MODIS to retrieve albedo and obtain cloud and surface classification mask.

between c and d?

Response:

Table 2 is included in the 'Data' section of the revised version to show the difference between the equipments and the matching models.

	Model 1		Model 2	
	λ range (nm)	validation data	λ range (nm)	validation data
Visible	300-700	/	400-700	albedometer
Near Infrared	700-2500	/	700-2100	albedometer
Shortwave	300-2500	pyranometer	400-2100	albedometer

Table 2: Difference between the two models mentioned in the text. Figures 3, 6 and Table A2 show retrieval and validation results of the two models.

Reviewer comment: Section 3.4: I don't understand the link between surface metamorphism and two days (Morning-noon-early afternoon, late afternoon) albedo changes. Figure 8 is not mentioned in section 3.4. If they have some links please elaborate more.

Response:

We appreciate your pointing out our omission of Figure 8 from the discussed text. In the revised version, the figure is referenced in the discussion context. In addition, the text below was added to Section 3.4 to provide more context.

Similar to how the Eulerian flow field is specified, the 'surface metamorphism' of sea ice can be studied by analyzing the albedo change at fixed locations. By subtracting the albedo on the first day from that at the same location on the following day, the albedo change over the last 24 hours due to metamorphism can be determined; a positive Δ_α at a fixed pixel indicates that the melt-pond (or open-water) has refrozen (or frozen), while a negative Δ_α indicates ice (or snow) has melted. Notably, the subtractions are carried out at similar solar zenith angles (morning to morning, noon to noon, etc.), which eliminates the effect of solar zenith angle on albedo change.

Reviewer comment: Section 3.5: The retrieved albedo using SGLI is also comprehensively validated like a MODIS and analyzed with solar zenith angle, surface metamorphism. The retrieved albedo using SGLI should be validated and compared in parallel.

Response:

The GCOM-C/SGLI was launched in 2019 and data from the AFLUX campaign (Figure 9) was the only validation data we could found. The purpose of including the results from SGLI is to show that the SciML/RTM framework (Fig. 1) is applicable to not just one sensor. Comprehensive validation of SGLI is beyond the scope of the current paper and is discussed in a separate work by comparing the retrieval results with MODIS in the Sea of Okhotsk Region.

Reviewer comment: Section 4.1 and 4.2: In 4.1, albedo retrieval map against MCD is daily but in 4.2, 5-day mean albedo map against MERIS. Can you elaborate why they are different?

Response:

As noted in line 36∼41, Qu and Peng retrieved sea-ice albedo using the direct estimation method. Initially, we intended to utilize Qu's results as a benchmark for comparing the three algorithms. However, because we were unable to obtain the authors' original retrieval data in order to include it in the subplot, we could only show three columns in Figure 13 by the time we submitted the first version. For your reference, Fig. 2 below shows the comparison of the three products, and the first column are screenshots of the results of Qu's algorithm, taken directly from their paper. For the second and third column, we used the same color-bar to plot the results and manually boxed the same area, but due to difference in printing and in coordinates, the colors/regions don't exactly match with panels (a) and (b).

Reviewer comment: The retrieved albedo maps are only shown near Svalbard islands but Pan-Arctic retrieved albedo map should be shown and have to be compared with other comparison dataset.

Response:

We appreciate this comment. A Pan-Arctic retrieval map will be used in the

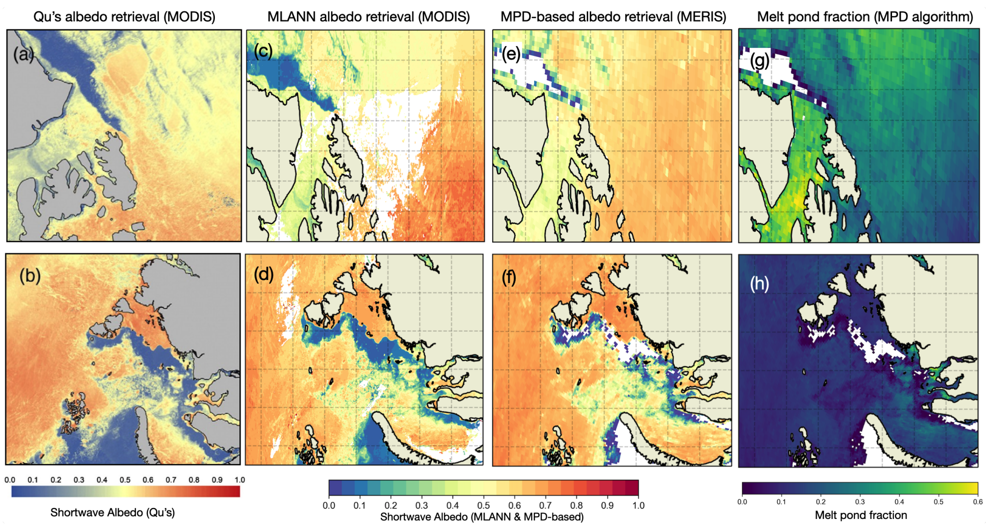

Figure 2: Maps of albedo and melt pond fraction averaged during a 5-day period in 2007 between DOY 166 and 170. From left to right: Qu's albedo retrievals, MLANN-based and MPD-based albedo retrievals, as well as the MPD-derived melt pond fraction, respectively (Qu2015Mapping, this study, and Istomina2015Melt). The upper panels depict the Banks, Prince Patrick, and Melville Islands, while the lower panels depict the Kara Sea. At the bottom, colorbars representing the corresponding values are displayed. Note that the images of Qu's retrieval results (along with the colorbar) are taken directly from Fig.10 in Qu2015Mapping, as no other data was obtainable. In panels (c) and (d), empty regions represent cloud pixels that were detected by the MLCM model (and hence removed), whereas empty regions in panels (e) through (h) represent either cloud pixels or open-water areas that were not processed by the MPD algorithm.

revised version.

1.2 Minor Comments

Reviewer comment: All captions in the table should be above table.
Response:
Done.

Reviewer comment: L 99, 100: Please mention SGLI MCD 43 full name
Response:
Revised. Second-generation Global Imager (SGLI), and Moderate Resolution Imaging Spectroradiometer (MODIS) MCD43D49, MCD43D50 and MCD43D51.

Reviewer comment: P4, L101-105: should go to the discussion section
Response:
Done.

Reviewer comment: 3 validaiton: The authors mentioned MOSAiC. Have you used the data from MOSAiC for the validation?
Response:
As described on line 304, "The MOSAiC campaign included fewer than 50 valid data points, and all obtained for broken cloud conditions. To eliminate errors caused by dense cloud cover, MOSAiC data were omitted from validation."

Reviewer comment: L 497-499: should go comparison dataset
Response:
Done.

Appendix

Parameter	Sym.	Unit	Value
Sea-ice thickness	h	m	$0 \sim 3$
Brine pocket volume fraction	V_{br}	$-$	$(-0.067 \cdot \log(h) + 0.1147) \cdot (1 + 0.2 \cdot r_{\mathrm{bu}})$
Brine pocket radius	r_{br}	μm	$300 \sim 700$
Air bubble volume fraction	V_{bu}	$-$	$0.0214 \cdot h + 0.0068$
Air bubble radius	r_{bu}	μm	$-18.3 \cdot h^2 + 222.7 \cdot h + 96.5$

Table 3: Physical parameters of ice. In generating the sea-ice thickness, a truncated-normal distribution with $\mu = 0.03$, $\sigma = 1.5$ was used to ensure an adequate amount of thin ice in the SD. The brine pocket radius conforms to a Tukey-Lamdba distribution with λ=0.5.

Parameter	Units	Value
Melt water thickness	m	$0 \sim 1.5$
Chlorophyll concentrations	mg/m^3	$0.5 \sim 10$
CDOM at 443 nm	/m	$0.01 \sim 0.1$

Table 4: Physical parameters of melt water on ice and ocean water. Melt water thickness and CDOM values follow randomly-distributed uniform distributions in the specified ranges. For the chl-a concentration, a reciprocal continuous distribution (long tail extending to high values) was used.

Parameter	Symbol	Units	Value
Snow grain size	r_{e}	μm	$50 \sim 150$
Snow density	ρ_s	kg/m^3	200
Impurity fractions	$\mathrm{f}_{\mathrm{imp}}$	-	$10^{-7} \sim 10^{-6}$
Snow thickness	h_{snow}	m	$0.01 \sim 0.2$

Table 5: Physical parameters of snow cover. The snow grain size and snow thickness were generated with a randomly uniform distribution in the specified ranges.

Parameters	Value
Solar zenith angle	20$\sim$80 degrees
Sensor angle	0.01$\sim$50 degrees
Azimuth angle	0.01$\sim$180 degrees
AOD at 500 nm	$0.01 \sim 0.3$
Relative humidity	0.5
Fine mode fraction	0.9

Table 6: Geometries and atmospheric parameters. All parameters conform to random-uniform distributions in the specified ranges.